NANO LETTERS

LETTER

pubs.acs.org/NanoLett

Micrometer-Scale Ballistic Transport in Encapsulated Graphene at Room Temperature

Alexander S. Mayorov,*[,†] Roman V. Gorbachev,[†] Sergey V. Morozov,[†,‡] Liam Britnell,[†] Rashid Jalil,[§] Leonid A. Ponomarenko,[†] Peter Blake,[§] Kostya S. Novoselov,[†] Kenji Watanabe,[∥] Takashi Taniguchi,[∥] and A. K. Geim[†,§]

[†]School of Physics and Astronomy, University of Manchester, Oxford Road, Manchester M13 9PL, United Kingdom

[‡]Institute for Microelectronics Technology, 142432 Chernogolovka, Russia

[§]Manchester Centre for Mesoscience and Nanotechnology, University of Manchester, Manchester M13 9PL, United Kingdom

[∥]National Institute for Materials Science, 1-1 Namiki, Tsukuba, 305-0044 Japan

ABSTRACT: Devices made from graphene encapsulated in hexagonal boron-nitride exhibit pronounced negative bend resistance and an anomalous Hall effect, which are a direct consequence of room-temperature ballistic transport at a micrometer scale for a wide range of carrier concentrations. The encapsulation makes graphene practically insusceptible to the ambient atmosphere and, simultaneously, allows the use of boron nitride as an ultrathin top gate dielectric.

KEYWORDS: Boron nitride, encapsulated graphene, ballistic transport, negative bend resistance, top gate

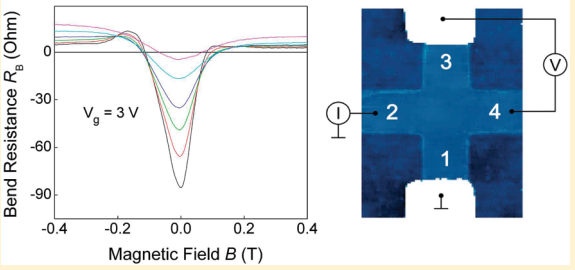

In search for new phenomena and applications, which are expected, predicted or to be uncovered in graphene, it is important to continue improving its electronic quality that is commonly characterized by charge carrier mobility μ. Graphene obtained by mechanical cleavage on top of an oxidized Si wafer usually exhibits $\mu \sim 10\,000$ cm^2 V^{-1} s^{-1}.[1] For typical carrier concentrations $n \approx 10^{12}$ cm^{-2}, such quality translates into the mean free path $l = (h/2e)\mu(n/\pi)^{0.5}$ of the order of 100 nm where h is Planck's constant and e is the electron charge. On the other hand, it has been shown that if extrinsic scattering in graphene is eliminated its mobility at room temperature (T) can reach $\sim$200 000 cm^2 V^{-1} s^{-1} due to weak electron−phonon interaction.[2] Indeed, for $n \sim 10^{11}$ cm^{-2} μ exceeding 100 000 cm^2 V^{-1} s^{-1} and 1 000 000 cm^2 V^{-1} s^{-1} at room and liquid-helium T, respectively, were demonstrated for suspended graphene annealed by high electric current.[3−5] However, suspended devices are extremely fragile, susceptible to the ambient atmosphere, and difficult to anneal in the proper four-probe geometry (the latter was not achieved so far). Furthermore, it requires a significant amount of strain to suppress flexural modes in suspended graphene and retain high μ up to room T.[5] Most recently, a breakthrough was achieved by using hexagonal boron-nitride (hBN) as an atomically smooth and inert substrate for cleaved graphene.[6] Such structures were shown to exhibit $\mu \sim 100\,000$ cm^2 V^{-1} s^{-1} at $n \sim 10^{11}$ cm^{-2}. Although μ achieved in graphene yield l approaching 1 μm, no ballistic effects on this scale have so far been reported.

In this Letter, we describe devices made from graphene sandwiched between two hBN crystals. The devices exhibit room-T ballistic transport well over a 1 μm distance, as evidenced directly from the negative transfer resistance measured in the bend geometry.[7] At low $n \sim 10^{11}$ cm^{-2}, the devices exhibit mobility $\mu > 100\,000$ cm^2 V^{-1} s^{-1} even at room T, as determined from their response to gate voltage.[1−6] At higher $n \approx 10^{12}$ cm^{-2}, we find that our devices' longitudinal conductivity σ becomes limited by their width $w \approx 1$ μm rather than scattering in the bulk. To extract intrinsic μ and l in this ballistic regime, we employed measurements of bend resistance R_B that, unlike σ, continues being sensitive to l. Our analysis yields $l \approx 3$ μm for $n \approx 10^{12}$ cm^{-2} and at low T, which translates into $\mu \sim 500\,000$ cm^2 V^{-1} s^{-1}. In addition, the encapsulation has made graphene insusceptible to the environment so that long and repeated exposure to the ambient air was found to have little effect on remnant doping and μ.

The studied samples that we further refer to as graphene-boron-nitride (GBN) heterostructures were fabricated by using the following multistep technology. First, relatively thick ($\sim$10 nm) hBN crystals were mechanically deposited on top of an oxidized Si wafer (100 nm of SiO_2). Then, submillimeter graphene crystallites were produced by cleavage on another substrate precoated with a double layer polymer stack. The bottom polymer "release" layer was then dissolved from the sides and the resulting film with the graphene flake was transferred on top of the chosen hBN crystal. Similarly to ref 8, we have found that to achieve high mobility it was important not to expose the graphene surface (that goes into contact with hBN) to any solvent (dry transfer technique). Electron-beam lithography and oxygen plasma etching were then employed to define graphene Hall bars (see images in Figures 1 and 2). The deposition of graphene on hBN

Received: March 7, 2011
Revised: April 26, 2011
Published: May 16, 2011

dx.doi.org/10.1021/nl200758b | *Nano Lett.* 2011, 11, 2396–2399

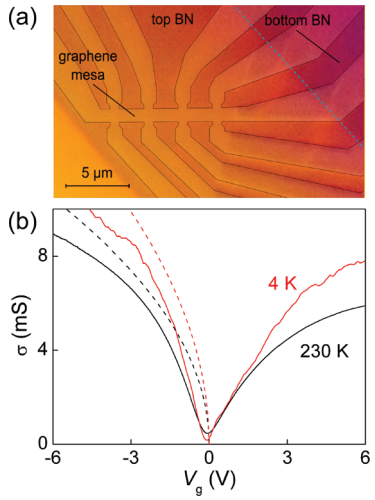

Figure 1. (a) Optical micrograph of one of our GBN devices. The plasma etching resulted in a few nanometers tall mesa that could be visualized by using the differential interference contrast. To improve the mesa's visibility, its contour is shown by the thin gray lines. The slanted dashed line indicates the edge of the top hBN crystal. (b) $\sigma(V_g)$ measured at two T (solid curves). The dashed curves are σ calculated by using the Landauer−Buttiker formula and numerical modeling of the transmission probability through a quantum wire with $w = 1$ μm. In the calculations, we assume diffusive boundary scattering and the intrinsic mean free path in the graphene bulk $l_i = 1.5$ and 3 μm at 230 and 4 K, respectively, which are the values inferred from measurements of R_B as described below. Note that the standard analysis for the extraction of the field-effect μ from $\sigma(n)$ is valid only for the diffusive regime and fails at higher n where $l > w$.

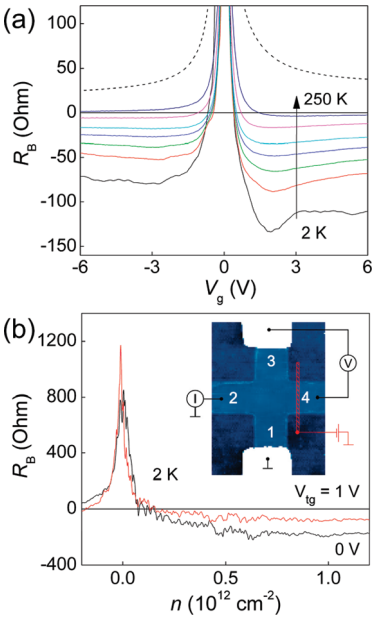

Figure 2. (a) Bend resistance at various T for the same device as in Figure 1b. The curves from bottom to top correspond to 2, 50, 80, 110, 140, 200, and 250 K, respectively. The dashed curve is R_B calculated using $\sigma(V_g)$ and the van der Pauw formula. (b) Inset: atomic force micrograph of one of our Hall crosses. The scale is given by the device width $w \approx 1$ μm. The drawings schematically depict the bend measurement geometry and a narrow top gate (in red) deposited across one of the leads at a later microfabrication stage. Main panel: $R_B(n)$ for a device with the such a top gate. The negative R_B can be suppressed by applying top-gate voltage V_{tg} which creates an extra barrier and reflects electrons.

resulted in numerous "bubbles" containing trapped adsorbates (presumably hydrocarbons), and if present in the active part of our devices such bubbles caused significant charge inhomogeneity. This limited the achievable w to ~1 μm, as we tried to fit the central wire inside areas free from the bubbles. The second hBN crystal (~10 nm thick) was again transferred by using the same dry procedure. The top crystal was carefully aligned to encapsulate the graphene Hall bar but leave the contact regions open for depositing metal (Au/Ti) contacts. In some devices, the top hBN crystal was used as a dielectric for local gating. After each transfer step, the devices were annealed at 300 °C in an argon−hydrogen atmosphere to remove polymer residues and other contamination.

Figure 1b shows σ as a function of back-gate voltage V_g for a GBN device, measured in the standard four-probe geometry. The minimum in σ occurs at $V_g \approx -0.1$ V, indicating little extrinsic doping (~10^{10} cm^{-2}). At small hole concentrations $n \sim 10^{11}$ cm^{-2}, the slopes of $\sigma(V_g)$ yield $\mu \approx 140\,000$ and 100 000 cm^2 V^{-1} s^{-1} at 4 K and near room T, respectively (low-n μ is about 30% lower for electrons). The values are in agreement with the measured Hall mobility. In general, at low n our GBN devices exhibited μ between 20 000 and 150 000 cm^2 V^{-1} s^{-1}, tending to ≈100 000 cm^2 V^{-1} s^{-1} in most cases. This translates into a submicrometer mean free path, that is, less than our devices' width ($w = 1$ μm), which justifies the use of the diffusive transport formulas at low n.

A notable feature of Figure 1b is a relatively weak T dependence of $\sigma(V_g)$ away from the neutrality point, which is surprising because electron−phonon scattering is expected to start playing a significant role in graphene of such quality.[2,5,9] Also, the strong sublinear behavior of $\sigma(V_g)$ is unusual for graphene measured in the four probe geometry. As shown below, these features are related to electron transport limited at high n by boundary scattering so that $\sigma = 2e^2/h(k_F l) \propto n^{1/2} \propto V_g^{1/2}$, where $l \sim w$ and, therefore, σ weakly depends on T. In the limit $l \geq w$, we cannot use the standard formulas to extract μ and l and a special care should be taken to interpret the $\sigma(n)$ behavior. The importance of boundary scattering in our devices can be immediately appreciated if we estimate transmission probability Tr through our 3 μm long device in Figure 1. To this end, the standard Landauer−Buttiker formula for quantum conductance $G = (4e^2/\pi h)(k_F w)$Tr yields at high n, Tr ≈ 0.4, which indicates quasi-ballistic transport (here, $k_F w/\pi$ is the number of propagating Dirac fermions modes).

To gain further information about electronic quality of the GBN bulk in the ballistic limit, we have studied bend resistance R_B.[10] To this end, we applied current I_{21} between contacts 2 and 1 and measured voltage V_{34} between probes 3 and 4 (see Figure 2), which yielded $R_B = R_{34,21} = V_{34}/I_{21}$. Different bend configurations (e.g., $R_{14,23}$ and $R_{32,14}$) yielded similar $R_B(V_g)$. For a diffusive conductor, R_B should be equal to $(\ln 2)/\pi\sigma$.[11] The van der Pauw formula uses the diffusive approximation and can accurately describe $R_B(V_g)$ in the standard-quality graphene.[10] However, the formalism completely fails in our high-μ devices. Indeed, R_B becomes negative, which shows that most of the charge carriers injected from, for example, contact 2 can reach contact 4 without being scattered. The counterintuitive negative resistance was observed in high-μ two-dimensional gases based on GaAlAs heterostructures and required $l_i \gg w$ where l_i is the mean free path in the bulk.[7] Such ballistic propagation of charge

dx.doi.org/10.1021/nl200758b |Nano Lett. 2011, 11, 2396–2399

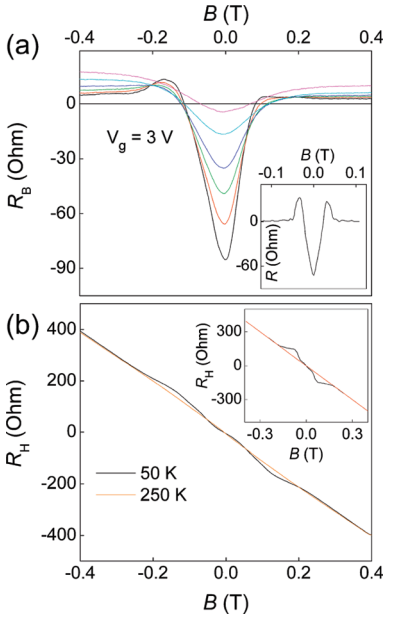

Figure 3. Ballistic transport in magnetic field. (a) $R_B(B)$ for a fixed $n \approx 6 \times 10^{11}$ cm^{-2}. T is 50, 80, 110, 140, 200, and 250 K (from bottom to top curves, respectively). Inset: $R_B(B)$ calculated for a Hall cross using the billiard-ball model[7] and scaled for the case of our graphene devices and the above n. (b) Hall resistance R_H measured at 50 and 250 K. Inset: $R_H(B)$ found theoretically for rounded corners[7] and scaled for our case. The red line in the inset indicates the diffusive limit.

carriers has not been reported in graphene before except for ref 12 where low-T nonlinear $I-V$ characteristics were measured in 50 nm Hall crosses at a fixed n and interpreted in terms of ballistic transport.

In contrast to the measurements in the standard geometry as in Figure 1b, R_B in Figure 2a exhibits very strong T dependence, which is in agreement with the expectations for high-μ graphene.[5,9] Despite this extra phonon scattering, R_B remains negative at high n for all $T \leq 250$ K (our highest T in the experimental setup) and does not even approach the gate dependence expected in the diffusive regime (dashed curve in Figure 2a). This observation yields $l_i > w \approx 1$ μm even at room T, which is the condition essential for the observation of negative R_B.[7,13] The strong T dependence of R_B also signifies that l_i grows substantially with decreasing T. Complementary evidence for ballistic transfer through the Hall cross comes from devices with an extra barrier placed across one of the potential leads (Figure 2b). When a voltage was applied to the narrow top gate, the potential barrier reflected some carriers back into the cross and, accordingly, suppressed negative R_B. Also, note that, in the low-n regime ($|V_g| < 0.5$ V) where we could determine μ from the linear dependence $\sigma \propto V_g$ as ~140 000 cm^2 V^{-1} s^{-1}, R_B remains positive, as expected, because the corresponding $l = (h/2e)\mu(n/\pi)^{0.5} \leq 0.5$ μm is insufficient for causing the ballistic conditions and negative R_B.

To elucidate the micrometer-scale ballistic transport in our GBN heterostructures, Figure 3a shows R_B as a function of magnetic field B applied perpendicular to graphene at a fixed V_g (+3 V in this case). As expected,[7] R_B changes its sign with increasing B because injected electrons are bended by B and can no longer reach the opposite contact ballistically. This behavior is in agreement with the one reported in GaAlAs heterostructures.[7,14] The characteristic field B_0 at which R_B changes sign in Figure 3a is ~0.1 T, which corresponds to a cyclotron orbit of radius $r_c = \hbar(\pi n)^{1/2}/eB \approx 1$ μm, that is equal to w, which is in agreement with theory[7,14] ($n \approx 6 \times 10^{11}$ cm^{-2} in this case). Furthermore, ballistic transport is expected to cause an anomalous behavior of Hall resistivity R_H such that it is no longer a linear function of B. Figure 3b shows that, indeed, our devices exhibit nonlinear $R_H(B)$ with a notable kink at the same characteristic B_0. This anomaly is usually referred to as the last plateau and absent in diffusive systems.[7] The kink almost disappears near room T (Figure 3b) indicating that we get closer to the diffusive regime. The functional form of $R_H(B)$ strongly depends on the exact shape of Hall crosses, and the anomaly becomes minor if a cross has sharp corners,[7,14] as is the case of our devices (see image in Figure 2b).

The negative R_B, its magnetic field behavior, anomalies in R_H, and the influence of the top gate unambiguously prove that in our Hall crosses charge carriers can reach the opposite lead ballistically without scattering. This yields l longer than 1 μm for all $|V_g| > 1$ V where the large negative R_B is observed ($|n| \geq 2 \times 10^{11}$ cm^{-2}). To appreciate such large values of l, let us mention that in suspended devices[3,4] and graphene on BN[6] ultrahigh μ were reported only at low $n \sim 10^{11}$ cm^{-2}, which translates into submicrometer l,[3,4] and $l \approx 1$ μm were achieved only in suspended devices with a million μ at low T.[5]

For $l_i > w$, the boundary scattering makes σ only weakly dependent on the bulk quality of graphene, and to obtain a better estimate for l_i than just ≥ 1 μm as above we used numerical simulations. We calculated R_B by using the billiard-ball model[7] and assuming diffusive boundary scattering. If the scattering is assumed specular, calculated R_B cannot reach the large negative values observed experimentally. This agrees with general expectations that etched graphene edges are usually rough and scatter diffusively. Diffusive boundary scattering decreases σ of a ballistic wire (transmission probability decreases) but makes R_B more negative due to collimation effects.[15] This is consistent with our experiment that shows higher (more ballistic) σ for holes but more negative R_B for electrons and vice versa (cf. Figures 1 and 2). This asymmetry can be attributed to a larger degree of diffusivity in boundary scattering for electrons, which implies an extra charge that breaks the electron−hole symmetry of the boundary. Under the assumption of diffusive scattering, the measured R_B yield $l_i \approx 1.5$ μm near room T and ≈3 μm below 50 K for $|n| > 2 \times 10^{11}$ cm^{-2} ($|V_g| > 1$ V). Although the exact values are inferred by and assuming diffusive boundaries, such large l_i (of the order of a couple of micrometers) are essential to explain qualitatively both large negative R_B and its strong T dependence (for example, $l_i \leq 1$ μm would be inconsistent with these observations). The inferred l_i also allow us to understand the behavior of σ and its weak T dependence, and the dashed curves in Figure 1b show $\sigma(V_g)$ calculated within the same model and parameters. Better agreement with the experiment could be achieved by modeling local doping profiles near edges but this goes beyond the accuracy of our simple billiard-ball model.

Finally, we note that for $n \approx 4 \times 10^{11}$ cm^{-2} where R_B reaches its most negative value $l_i \approx 3$ μm implies intrinsic $\mu \sim$ 500 000 cm^2 V^{-1} s^{-1}. It is an extremely high value for graphene but without it we would not be able to observe large negative R_B. Note that this is also consistent with $\mu \sim 150\,000$ cm^2 V^{-1} s^{-1} found from the standard field effect analysis at lower $n \approx 1 \times 10^{11}$ cm^{-2} where charge inhomogeneity remains significant. The latter regime corresponds to $l_i \leq 0.5$ μm and does not allow

dx.doi.org/10.1021/nl200758b |Nano Lett. 2011, 11, 2396–2399

negative R_B at low n, which is in agreement in the experimental observations. To confirm the ultrahigh μ at high n by using the analysis of $\sigma(n)$, which has become conventional for graphene, would require GBN devices with $w > 5\ \mu$m (diffusive regime). So far, we have been unable to achieve this because of the mentioned bubbles that result in charge inhomogeneity.

In conclusion, graphene encapsulated in hBN exhibits robust ballistic transport with a large negative transfer resistance and the mean free path exceeding ~3 μm at low T. Away from the neutrality point, (for carrier concentrations above 10^{11} cm^{-2}) the longitudinal conductivity of our 1 μm wide devices becomes limited by diffusive scattering at the sample boundaries rather than in the graphene bulk. The demonstrated graphene-boron-nitride heterostructures is a further improvement with respect to the devices reported previously, in terms of their environmental stability and the possibility of using the encapsulating hBN as a quality top dielectric. Our work also shows that it should be possible to achieve million mobilities for graphene on boron nitride.

AUTHOR INFORMATION

Corresponding Author

*E-mail: mayorov@gmail.com.

ACKNOWLEDGMENT

This work was supported by the Körber Foundation, Engineering and Physical Sciences Research Council (U.K.), the Office of Naval Research, the Air Force Office of Scientific Research, and the Royal Society.

REFERENCES

(1) Geim, A. K.; Novoselov, K. S. The rise of graphene. *Nat. Mater.* **2007**, *6*, 183–191.

(2) Morozov, S. V.; Novoselov, K. S.; Katsnelson, M. I.; Schedin, F.; Elias, D. C.; Jaszczak, J. A.; Geim, A. K. Giant intrinsic carrier mobilities in graphene and its bilayer. *Phys. Rev. Lett.* **2008**, *100*, 016602.

(3) Du, X.; Skachko, I.; Barker, A.; Andrei, E. Y. Approaching ballistic transport in suspended graphene. *Nat. Nanotechnol.* **2008**, *3*, 491–495.

(4) Bolotin, K. I.; Sikes, K. J.; Hone, J.; Stormer, H. L.; Kim, P. Temperature-dependent transport in suspended graphene. *Phys. Rev. Lett.* **2008**, *101*, 096802.

(5) Castro, E. V.; Ochoa, H.; Katsnelson, M. I.; Gorbachev, R. V.; Elias, D. C.; Novoselov, K. S.; Geim, A. K.; Guinea, F. Limits on charge carrier mobility in suspended graphene due to flexural phonons. *Phys. Rev. Lett.* **2010**, *105*, 266601.

(6) Dean, C. R.; Young, A. F.; Meric, I.; Lee, C.; Wang, L.; Sorgenfrei, S.; Watanabe, K.; Taniguchi, T.; Kim, P.; Shepard, K. L.; Hone, J. Boron nitride substrates for high-quality graphene electronics. *Nat. Nanotechnol.* **2010**, *5*, 722–726.

(7) Beenakker, C. W. J.; van Houten, H. Billiard model of a ballistic multiprobe conductor. *Phys. Rev. Lett.* **1989**, *63*, 1857–1860.

(8) Dean, C. R.; Young, A. F.; Cadden-Zimansky, P.; Wang, L.; Ren, H.; Watanabe, K.; Taniguchi, T.; Kim, P.; Hone, J.; Shepard, K. L. *Multicomponent fractional quantum Hall effect in graphene*. arXiv:1010.1179, 2010.

(9) Hwang, E. H.; Das Sarma, S. Acoustic phonon scattering limited carrier mobility in two-dimensional extrinsic graphene. *Phys. Rev. B* **2008**, *77*, 115449.

(10) Blake, P.; Yang, R.; Morozov, S. V.; Schedin, F.; Ponomarenko, L. A.; Zhukov, A. A.; Grigorieva, I. V.; Novoselov, K. S.; Geim, A. K. Influence of metal contacts and charge inhomogeneity on transport properties of graphene near the neutrality point. *Solid State Commun.* **2009**, *149*, 1068–1071.

(11) van der Pauw, L. J. A method of measuring the resistivity and Hall coefficient on lamellae of arbitrary shape. *Philips Tech. Rev.* **1958**, *20*, 220–224.

(12) Weingart, S.; Bock, C.; Kunze, U.; Speck, F.; Seyller, Th.; Ley, L. Low-temperature ballistic transport in nanoscale epitaxial graphene cross junctions. *Appl. Phys. Lett.* **2009**, *95*, 262101.

(13) Gilbertson, A. M.; Fearn, M.; Kormányos, A.; Read, D. E.; Emeny, M. T.; Lambert, C. J.; Ashley, T.; Solin, S. A.; Cohen, L. F. Ballistic transport and boundary scattering in InSb/InxAl1-xSb mesoscopic devices. *Phys. Rev. B* **2011**, *83*, 075304.

(14) Timp, G.; Baranger, H. U.; de Vegvar, P.; Cunningham, J. E.; Howard, R. E.; Behringer, R.; Mankiewich, P. M. Propagation around a bend in a multichannel electron waveguide. *Phys. Rev. Lett.* **1988**, *60*, 2081–2084.

(15) Blaikie, R. J.; Nakazato, J. R. A.; Cleaver, H. Ahmed. Enhancement of resistance anomalies by diffuse boundary scattering in multiprobe ballistic conductors. *Phys. Rev. B* **1992**, *46*, 9796–9799.